3D-printed metasurfaces of capped helices providing broadband negative mode index

P. Petrov[1], A. P. Hibbins[1], N. Aboulkhair[2], E.Saleh[3] and J. R. Sambles[1]

[1] University of Exeter, Department of Physics and Astronomy, EX4 4QL, Exeter, United Kingdom
[2] University of Nottingham, Faculty of Engineering, NG8 1BB, Nottingham, United Kingdom
[3] University of Leeds, Faculty of Engineering, LS2 9JT, Leeds, United Kingdom
pp386@exeter.ac.uk

Abstract – **Using structures of subwavelength metallic capped helices with both negative electric and magnetic couplings, we demonstrate a broadband negative mode index metasurface. Numerical and experimental results are presented for the structure with negative dispersion bandwidth of 44% compared to the resonant frequency of individual capped helices. Optimisation of such structures in terms of their size, element geometry and operational passband width is demonstrated.**

I. Introduction

Negative refractive index materials were first theoretically proposed in the work of V. Veselago [1] as those that possess simultaneously negative electric permittivity (ε) and magnetic permeability (μ). Waves that propagate in any medium characterized by a negative refractive index have wave-fronts (k) that move in the opposite direction to the energy flow (S). The possibility of realising such material was suggested in the works of Sir J.B. Pendry and co-workers [2], who proposed a structure that combines negatively magnetically coupled meta-atoms [3] together with metallic rods that operate below their effective plasma frequency [4]. The experimental realisation of negative index propagation in these structures was demonstrated by D.R. Smith et al [5]. Different geometries of meta-atoms have been studied since then including split ring resonators (SRRs) [5, 6], Swiss rolls [7] and helices [8]. Negative index structures have been demonstrated for frequency ranges from microwave [5-8] to infrared [9-10].

One can also study the negative index propagation of modes on structured surfaces and the 'Sievenpiper mushroom' structure [11] which is a well-known example of such a metasurface. While originally studied to offer an artificial magnetic conductor (AMC) boundary condition for antenna systems, it has also been demonstrated to support negative mode index for surface waves across a narrow bandwidth [12]. It was shown that negative index structures can be useful for such applications as perfect lenses [13], cloaking devises [14] and in the wavelength division multiplex (WDM) systems based on negative index metamaterials [15].

Although a variety of approaches and geometries have been proposed over the last decades, the general drawback of such structures has been the narrow operational bandwidths. The widest operational band, to the best of our knowledge has been reported in [13] where about 20% bandwidth compared to the resonant frequency has been achieved.

An array of helices, with axes arranged parallel to each other and orthogonal to a ground plane, provides negative coupling between them. This results in negative dispersion which was demonstrated in [8]. If conductive 'caps' are placed on the top of these helices, the coupling may also become electric but it should still be possible to observe the negative mode index as in mushroom structures [12]. In this work we explore a structure of capped helices that combines negative magnetic and electric couplings. As a result, this strong subwavelength structure provides an extremely broad negative index mode that is significantly wider than those presented in the literature when compared to their wavelength. In addition we discuss the possible ways to broaden the negative index band even further.

II. Surface of Capped Helices

To realise both negative electric and magnetic couplings in the array of capped helices we propose the structure demonstrated on Fig. 1 (a). The holes in the metal caps are left in order to minimise the magnetic field shielding and thereby conserve the magnetic coupling provided by the array of helices. A hexagonal geometry is chosen in order to provide a near isotropic in-plane response and the ground plane has been introduced to simplify the assembly of the elements.

The structure has been 3D-printed using selective laser melting (SLM) of a titanium alloy (Ti 6Al-4V). The resistivity of the printed structure $\rho = 1.12 \pm 0.02$ μΩm was determined based on measuring a 30 x 1 x 1 mm bar built using the same SLM process and material, using Keithley high precision multimeter. Helices have been manufactured in groups of 7 in a hexagonal arrangement as shown on Fig. 1 (b), and then assembled into the 2D array. Parameters of the helices as given in Fig. 1(a) are: outer diameter of helices D = 2.6 mm, diameter of holes d = 1.2 mm, width of holes and

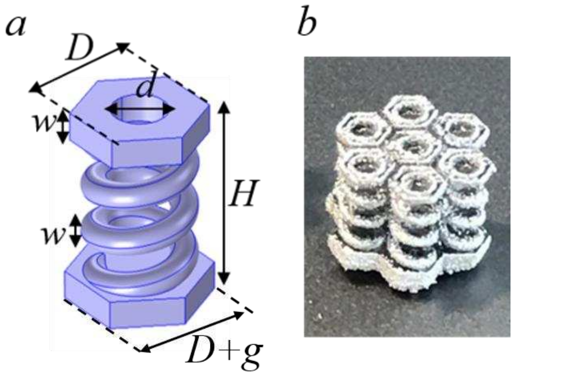

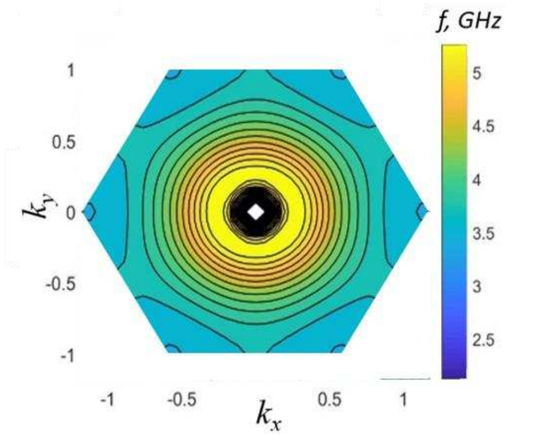

Fig.1. Left: COMSOL model for the unit cell of the capped helix array. D = 2.6 mm, d = 1.2 mm, w = 0.65, H = 4.5 mm.
Right: photo of 3D printed structure composed of 7 capped helices.

Fig.2. Numerical equienergy contours for surface modes supported by the capped helices structure. Unit cell presented on Fig.1.

helix wires w = 0.65, height of the structure H = 4.5 mm, number of turns n = 3.5. Helices have been arranged on the ground plane so that the distance between the top caps g = 0.2 mm. The resulting size of the unit cell in this case is $D + g$ = 2.8 mm. These parameters have been chosen to provide the widest possible operational band of the negative index surface mode, while taking into account the manufacturing limitations. It is also important to note that the structure is subwavelength with the height comprising from 5.1 to 8.1% of the wavelength at operational frequencies.

Numerical results for the dispersion of such structure have been obtained using finite element method (FEM) numerical simulations in COMSOL Multiphysics package. In Fig. 2 one can see that 2 waves are going to propagate in this structure: a forward one that goes follows closely the light line and a negative index surface wave over the frequency range between 3.4 and 5.4 GHz. This frequency range comprise 44% of the resonant frequency of individual helix, f_0 = 4.5 GHz, which is, to the best of our knowledge, the widest one reported in the literature. As the structure has hexagonal symmetry so does the dispersion, however the response is nearly isotropic-in-the-plane at almost all operational frequencies.

In order to experimentally determine the eigenmodes of the structure we have arranged a linear array of 20 elements (schematically shown on the insert of Fig.3). Instantaneous electric field profile of the surface waves that are excited from a point probe source located at the edge of the sample have been measured using the nearfield electric probe positioned at 0.2 mm distance above the top of the caps at the frequency range between 2 and 6 GHz. The probes have been connected to port 1 and port 2 of a vector network analyser. Fourier transform

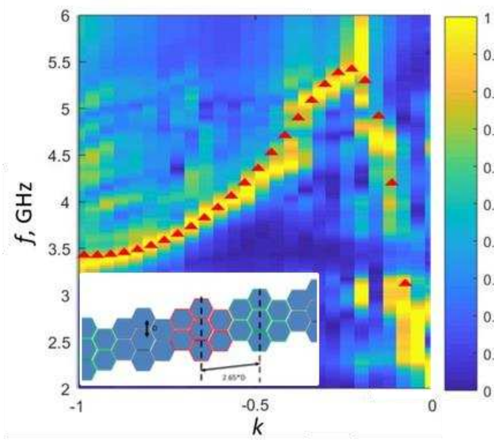

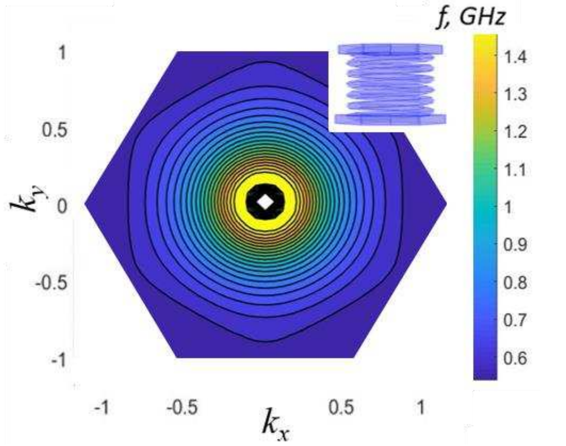

Fig. 3. Normalised experimental and numerical (red triangles) results for the 1st Brillouin zone backward wave dispersion in the chain of capped helices shown on the insert.

Fig. 4. Numerical equienergy contours for surface modes supported by the capped helices structure with increased bandwidth. Unit cell presented on the insert.

is then performed upon this spatial electric field distribution, with the magnitude of the Fourier terms indicative of the wave vector components strength present in the spatial field measurement. Experimental and numerical results for the backward wave dispersion are shown to be in the good agreement with each other (Fig. 3). The band splitting at negative wave dispersion that can be observed at 4.7GHz correspond to the large scale (2.65D) periodicity of our structure.

In order to maximise the bandwidth even further, both electric and magnetic couplings between elements should be increased. In order to increase the magnetic coupling, magnetic flux overlap between helices should be maximised. For that we should make the outer diameter of helices larger, and reduce the helix wire diameter. To maximise the electric coupling the gaps between elements should be made as small as possible compared to the wavelength. For instance numerical modelling has suggested that an improved capped-helix structure (shown on Fig.4) with n = 6, D = H = 4.5 mm, d = 1mm and g = 0.1 mm, supports a negative index surface mode with the operational band from 0.57 to 1.53 GHz, that is 83% of the resonant frequency.

CONCLUSIONS

A metasurface comprised of capped helices that supports a broadband negative-index surface-waves has been demonstrated numerically and experimentally between 3.4 and 5.4 GHz representing an operational band of 44% of the resonant frequency of individual element. This is more than double the bandwidth of that of structures previously reported in literature [16]. Suggestions are offered for ways to widen the operational band even further, with a specific geometry offering 83% bandwidth have been demonstrated.

ACKNOWLEDGEMENT

We acknowledge financial support from the Engineering and Physical Sciences Research Council (EPSRC) of the United Kingdom via the EPSRC Centre for Doctoral Training in Metamaterials (Grant No. EP/L015331/1). We also acknowledge financial support from the Defence Science and Technology Laboratory (Dstl) (Contract No: DSTLX1000133579). All data created during this research are openly available from the University of Exeter’s institutional repository at https://ore.exeter.ac.uk/.

REFERENCES

1 V. G. Veselago, The electrodynamics of substances with simultaneously negative values of permittivity and permeability, Soviet Physics Uspekhi 10, 4, (1968).
2 J. B. Pendry, A. J. Holdenz, D. J. Robbinsz, and W. J. Stewartz, Low frequency plasmons in thin-wire structures, J. Phys. Condens. Matter., 10, (1998).
3 J. B. Pendry, A. J. Holden, D. J. Robbins, and W. J. Stewart, Magnetism from conductors and enhanced nonlinear phenomena, IEEE Trans. Microwave Theory Techniq. 47, 11, (1999).
4 J. B. Pendry, Negative refraction makes a perfect lens, Phys. Rev. Lett. 85, 18, (2000).
5 D. R. Smith, W. J. Padilla, D. C. Vier, S. C. Nemat-Nasser, and S. Schultz, Composite medium with simultaneously negative permeability and permittivity, Phys. Rev. Lett. 84, 18, (2000).
6 R. A. Shelby, D. R. Smith, and S. Schultz, Experimental verification of a negative index of refraction, Science, 292, (2001).
7 M. C. K. Wiltshire, J. B. Pendry, I. R. Young, D. J. Larkman, D. J. Gilderdale, and J. V. Hajnal, Microstructured magnetic materials for RF flux guides in magnetic resonance imaging, Science 291 (2001).
8 H. Li, C. T. Chan, Theory and Experimental Realization of Negative Refraction in a Metallic Helix Array, Phys. Rev. Lett., 105, 247401, (2010)
9 U. K. Chettiar, A. V. Kildishev, H. K. Yuan, W. Cai, S. Xiao, V. P. Drachev, and V. M. Shalaev, Dual-band negative index metamaterial: double negative at 813 nm and single negative at 772 nm, Opt. Lett. 32 (2007).
10 J. Valentine, S. Zhang, T. Zentgraf, E. Ulin-Avila, D. A. Genov, G. Bartal, and X. Zhang, Three-dimensional optical metamaterial with a negative refractive index, Nature 455 (2008).
11 Sievenpiper, D. et al., High-Impedance Electromagnetic Surfaces with a Forbidden Frequency Band. IEEE T. Microw. Theory 47, 2059 (1999).
12 Dockrey, J. A. et al., Direct observation of negative-index microwave surface waves. Sci. Rep. 6, 22018, (2016).
13 Pendry, J. B., Negative refraction makes a perfect lens, Phys. Rev. Lett., 85, 3966–3969, (2000).
14 Bouchitt´e, G. and Schweizer, B., Cloaking of small objects by anomalous localized resonance, Quart. J. Mech. Appl. Math., 63, 437–463, (2010).
15 R. Yang, J. Wang, Broadband Microwave Negative Index Metamaterial with Low Dispersion, IEEE MTTS International Conference on Numerical Electromagnetic and Multiphysics Modeling and Optimization (NEMO), (2016).